

Search for a dijet resonance in events with jets and missing transverse energy in $p\bar{p}$ collisions at $\sqrt{s} = 1.96$ TeV

T. Aaltonen,²¹ S. Amerio^{jj,39} D. Amidei,³¹ A. Anastassov^{v,15} A. Annovi,¹⁷ J. Antos,¹² G. Apollinari,¹⁵ J.A. Appel,¹⁵ T. Arisawa,⁵² A. Artikov,¹³ J. Asaadi,⁴⁷ W. Ashmanskas,¹⁵ B. Auerbach,² A. Aurisano,⁴⁷ F. Azfar,³⁸ W. Badgett,¹⁵ T. Bae,²⁵ A. Barbaro-Galtieri,²⁶ V.E. Barnes,⁴³ B.A. Barnett,²³ P. Barria^{ll,41} P. Bartos,¹² M. Bauce^{jj,39} F. Bedeschi,⁴¹ S. Behari,¹⁵ G. Bellettini^{kk,41} J. Bellinger,⁵⁴ D. Benjamin,¹⁴ A. Beretvas,¹⁵ A. Bhatti,⁴⁵ K.R. Bland,⁵ B. Blumenfeld,²³ A. Bocci,¹⁴ A. Bodek,⁴⁴ D. Bortoletto,⁴³ J. Boudreau,⁴² A. Boveia,¹¹ L. Brigliadori^{ii,6} C. Bromberg,³² E. Brucken,²¹ J. Budagov,¹³ H.S. Budd,⁴⁴ K. Burkett,¹⁵ G. Busetto^{jj,39} P. Bussey,¹⁹ P. Butti^{kk,41} A. Buzatu,¹⁹ A. Calamba,¹⁰ S. Camarda,⁴ M. Campanelli,²⁸ F. Canelli^{cc,11} B. Carls,²² D. Carlsmith,⁵⁴ R. Carosi,⁴¹ S. Carrillo^{l,16} B. Casal^{j,9} M. Casarsa,⁴⁸ A. Castro^{ii,6} P. Catastini,²⁰ D. Cauz^{qrrr,48} V. Cavaliere,²² M. Cavalli-Sforza,⁴ A. Cerri^{e,26} L. Cerrito^{q,28} Y.C. Chen,¹ M. Chertok,⁷ G. Chiarelli,⁴¹ G. Chlachidze,¹⁵ K. Cho,²⁵ D. Chokheli,¹³ A. Clark,¹⁸ C. Clarke,⁵³ M.E. Convery,¹⁵ J. Conway,⁷ M. Corbo^{y,15} M. Cordelli,¹⁷ C.A. Cox,⁷ D.J. Cox,⁷ M. Cremonesi,⁴¹ D. Cruz,⁴⁷ J. Cuevas^{x,9} R. Culbertson,¹⁵ N. d'Ascenzo^{u,15} M. Datta^{ff,15} P. de Barbaro,⁴⁴ L. Demortier,⁴⁵ M. Deninno,⁶ M. D'Errico^{jj,39} F. Devoto,²¹ A. Di Canto^{kk,41} B. Di Ruzza^{p,15} J.R. Dittmann,⁵ S. Donati^{kk,41} M. D'Onofrio,²⁷ M. Dorigo^{ss,48} A. Driutti^{qrrr,48} K. Ebina,⁵² R. Edgar,³¹ A. Elagin,⁴⁷ R. Erbacher,⁷ S. Errede,²² B. Esham,²² S. Farrington,³⁸ J.P. Fernández Ramos,²⁹ R. Field,¹⁶ G. Flanagan^{s,15} R. Forrest,⁷ M. Franklin,²⁰ J.C. Freeman,¹⁵ H. Frisch,¹¹ Y. Funakoshi,⁵² C. Galloni^{kk,41} A.F. Garfinkel,⁴³ P. Garosi^{ll,41} H. Gerberich,²² E. Gerchtein,¹⁵ S. Giagu,⁴⁶ V. Giakoumopoulou,³ K. Gibson,⁴² C.M. Ginsburg,¹⁵ N. Giokaris,³ P. Giromini,¹⁷ G. Giurgiu,²³ V. Glagolev,¹³ D. Glenzinski,¹⁵ M. Gold,³⁴ D. Goldin,⁴⁷ A. Golossanov,¹⁵ G. Gomez,⁹ G. Gomez-Ceballos,³⁰ M. Goncharov,³⁰ O. González López,²⁹ I. Gorelov,³⁴ A.T. Goshaw,¹⁴ K. Goulianos,⁴⁵ E. Gramellini,⁶ S. Grinstein,⁴ C. Grosso-Pilcher,¹¹ R.C. Group,^{51,15} J. Guimaraes da Costa,²⁰ S.R. Hahn,¹⁵ J.Y. Han,⁴⁴ F. Happacher,¹⁷ K. Hara,⁴⁹ M. Hare,⁵⁰ R.F. Harr,⁵³ T. Harrington-Taber^{m,15} K. Hatakeyama,⁵ C. Hays,³⁸ J. Heinrich,⁴⁰ M. Herndon,⁵⁴ A. Hocker,¹⁵ Z. Hong,⁴⁷ W. Hopkins^{f,15} S. Hou,¹ R.E. Hughes,³⁵ U. Husemann,⁵⁵ M. Hussein^{aa,32} J. Huston,³² G. Introzzi^{nnoo,41} M. Iori^{pp,46} A. Ivanov^{o,7} E. James,¹⁵ D. Jang,¹⁰ B. Jayatilaka,¹⁵ E.J. Jeon,²⁵ S. Jindariani,¹⁵ M. Jones,⁴³ K.K. Joo,²⁵ S.Y. Jun,¹⁰ T.R. Junk,¹⁵ M. Kambeitz,²⁴ T. Kamon,^{25,47} P.E. Karchin,⁵³ A. Kasmi,⁵ Y. Kato^{n,37} W. Ketchum^{gg,11} J. Keung,⁴⁰ B. Kilminster^{cc,15} D.H. Kim,²⁵ H.S. Kim,²⁵ J.E. Kim,²⁵ M.J. Kim,¹⁷ S.H. Kim,⁴⁹ S.B. Kim,²⁵ Y.J. Kim,²⁵ Y.K. Kim,¹¹ N. Kimura,⁵² M. Kirby,¹⁵ K. Knoepfel,¹⁵ K. Kondo,^{52,*} D.J. Kong,²⁵ J. Konigsberg,¹⁶ A.V. Kotwal,¹⁴ M. Kreps,²⁴ J. Kroll,⁴⁰ M. Kruse,¹⁴ T. Kuhr,²⁴ M. Kurata,⁴⁹ A.T. Laasanen,⁴³ S. Lammel,¹⁵ M. Lancaster,²⁸ K. Lannon^{w,35} G. Latino^{ll,41} H.S. Lee,²⁵ J.S. Lee,²⁵ S. Leo,⁴¹ S. Leone,⁴¹ J.D. Lewis,¹⁵ A. Limosani^{r,14} E. Lipeles,⁴⁰ A. Lister^{a,18} H. Liu,⁵¹ Q. Liu,⁴³ T. Liu,¹⁵ S. Lockwitz,⁵⁵ A. Loginov,⁵⁵ D. Lucchesi^{jj,39} A. Lucà,¹⁷ J. Lueck,²⁴ P. Lujan,²⁶ P. Lukens,¹⁵ G. Lungu,⁴⁵ J. Lys,²⁶ R. Lysak^{d,12} R. Madrak,¹⁵ P. Maestro^{ll,41} S. Malik,⁴⁵ G. Manca^{b,27} A. Manousakis-Katsikakis,³ L. Marchese^{hh,6} F. Margaroli,⁴⁶ P. Marino^{mm,41} M. Martínez,⁴ K. Matera,²² M.E. Mattson,⁵³ A. Mazzacane,¹⁵ P. Mazzanti,⁶ R. McNulty^{i,27} A. Mehta,²⁷ P. Mehtala,²¹ C. Mesropian,⁴⁵ T. Miao,¹⁵ D. Mietlicki,³¹ A. Mitra,¹ H. Miyake,⁴⁹ S. Moed,¹⁵ N. Moggi,⁶ C.S. Moon^{y,15} R. Moore^{ddee,15} M.J. Morello^{mm,41} A. Mukherjee,¹⁵ Th. Muller,²⁴ P. Murat,¹⁵ M. Mussini^{ii,6} J. Nachtman^{m,15} Y. Nagai,⁴⁹ J. Naganoma,⁵² I. Nakano,³⁶ A. Napier,⁵⁰ J. Nett,⁴⁷ C. Neu,⁵¹ T. Nigmanov,⁴² L. Nodulman,² S.Y. Noh,²⁵ O. Norniella,²² L. Oakes,³⁸ S.H. Oh,¹⁴ Y.D. Oh,²⁵ I. Oksuzian,⁵¹ T. Okusawa,³⁷ R. Orava,²¹ L. Ortolan,⁴ C. Pagliarone,⁴⁸ E. Palencia^{e,9} P. Palni,³⁴ V. Papadimitriou,¹⁵ W. Parker,⁵⁴ G. Pauletta^{qrrr,48} M. Paulini,¹⁰ C. Paus,³⁰ T.J. Phillips,¹⁴ G. Piacentino,⁴¹ E. Pianori,⁴⁰ J. Pilot,⁷ K. Pitts,²² C. Plager,⁸ L. Pondrom,⁵⁴ S. Poprocki^{f,15} K. Potamianos,²⁶ A. Pranko,²⁶ F. Prokoshin^{z,13} F. Ptohos^{g,17} G. Punzi^{kk,41} N. Ranjan,⁴³ I. Redondo Fernández,²⁹ P. Renton,³⁸ M. Rescigno,⁴⁶ F. Rimondi,^{6,*} L. Ristori,^{41,15} A. Robson,¹⁹ T. Rodriguez,⁴⁰ S. Rolli^{h,50} M. Ronzani^{kk,41} R. Roser,¹⁵ J.L. Rosner,¹¹ F. Ruffini^{ll,41} A. Ruiz,⁹ J. Russ,¹⁰ V. Rusu,¹⁵ W.K. Sakumoto,⁴⁴ Y. Sakurai,⁵² L. Santi^{qrrr,48} K. Sato,⁴⁹ V. Saveliev^{u,15} A. Savoy-Navarro^{y,15} P. Schlabach,¹⁵ E.E. Schmidt,¹⁵ T. Schwarz,³¹ L. Scodellaro,⁹ F. Scuri,⁴¹ S. Seidel,³⁴ Y. Seiya,³⁷ A. Semenov,¹³ F. Sforza^{kk,41} S.Z. Shalhout,⁷ T. Shears,²⁷ P.F. Shepard,⁴² M. Shimojima^{t,49} M. Shochet,¹¹ I. Shreyber-Tecker,³³ A. Simonenko,¹³ K. Sliwa,⁵⁰ J.R. Smith,⁷ F.D. Snider,¹⁵ H. Song,⁴² V. Sorin,⁴ R. St. Denis,¹⁹ M. Stancari,¹⁵ D. Stentz^{v,15} J. Strologas,³⁴ Y. Sudo,⁴⁹ A. Sukhanov,¹⁵ I. Suslov,¹³ K. Takemasa,⁴⁹ Y. Takeuchi,⁴⁹ J. Tang,¹¹ M. Tecchio,³¹ P.K. Teng,¹ J. Thom^{f,15} E. Thomson,⁴⁰ V. Thukral,⁴⁷ D. Toback,⁴⁷ S. Tokar,¹² K. Tollefson,³² T. Tomura,⁴⁹ D. Tonelli^{e,15} S. Torre,¹⁷ D. Torretta,¹⁵ P. Totaro,³⁹ M. Trovato^{mm,41} F. Ukegawa,⁴⁹ S. Uozumi,²⁵ F. Vázquez^{l,16} G. Velev,¹⁵ C. Vellidis,¹⁵ C. Vernieri^{mm,41} M. Vidal,⁴³ R. Vilar,⁹ J. Vizán^{bb,9} M. Vogel,³⁴ G. Volpi,¹⁷ P. Wagner,⁴⁰ R. Wallny^{j,15} S.M. Wang,¹ D. Waters,²⁸

W.C. Wester III,¹⁵ D. Whiteson^{c,40} A.B. Wicklund,² S. Wilbur,⁷ H.H. Williams,⁴⁰ J.S. Wilson,³¹ P. Wilson,¹⁵
 B.L. Winer,³⁵ P. Wittich^{f,15} S. Wolbers,¹⁵ H. Wolfe,³⁵ T. Wright,³¹ X. Wu,¹⁸ Z. Wu,⁵ K. Yamamoto,³⁷
 D. Yamato,³⁷ T. Yang,¹⁵ U.K. Yang,²⁵ Y.C. Yang,²⁵ W.-M. Yao,²⁶ G.P. Yeh,¹⁵ K. Yi^{m,15} J. Yoh,¹⁵
 K. Yorita,⁵² T. Yoshida^{k,37} G.B. Yu,¹⁴ I. Yu,²⁵ A.M. Zanetti,⁴⁸ Y. Zeng,¹⁴ C. Zhou,¹⁴ and S. Zucchelliⁱⁱ⁶
 (CDF Collaboration)[†]

¹*Institute of Physics, Academia Sinica, Taipei, Taiwan 11529, Republic of China*

²*Argonne National Laboratory, Argonne, Illinois 60439, USA*

³*University of Athens, 157 71 Athens, Greece*

⁴*Institut de Física d'Altes Energies, ICREA, Universitat Autònoma de Barcelona, E-08193, Bellaterra (Barcelona), Spain*

⁵*Baylor University, Waco, Texas 76798, USA*

⁶*Istituto Nazionale di Fisica Nucleare Bologna, ⁱⁱUniversity of Bologna, I-40127 Bologna, Italy*

⁷*University of California, Davis, Davis, California 95616, USA*

⁸*University of California, Los Angeles, Los Angeles, California 90024, USA*

⁹*Instituto de Física de Cantabria, CSIC-University of Cantabria, 39005 Santander, Spain*

¹⁰*Carnegie Mellon University, Pittsburgh, Pennsylvania 15213, USA*

¹¹*Enrico Fermi Institute, University of Chicago, Chicago, Illinois 60637, USA*

¹²*Comenius University, 842 48 Bratislava, Slovakia; Institute of Experimental Physics, 040 01 Kosice, Slovakia*

¹³*Joint Institute for Nuclear Research, RU-141980 Dubna, Russia*

¹⁴*Duke University, Durham, North Carolina 27708, USA*

¹⁵*Fermi National Accelerator Laboratory, Batavia, Illinois 60510, USA*

¹⁶*University of Florida, Gainesville, Florida 32611, USA*

¹⁷*Laboratori Nazionali di Frascati, Istituto Nazionale di Fisica Nucleare, I-00044 Frascati, Italy*

¹⁸*University of Geneva, CH-1211 Geneva 4, Switzerland*

¹⁹*Glasgow University, Glasgow G12 8QQ, United Kingdom*

²⁰*Harvard University, Cambridge, Massachusetts 02138, USA*

²¹*Division of High Energy Physics, Department of Physics, University of Helsinki,*

FIN-00014, Helsinki, Finland; Helsinki Institute of Physics, FIN-00014, Helsinki, Finland

²²*University of Illinois, Urbana, Illinois 61801, USA*

²³*The Johns Hopkins University, Baltimore, Maryland 21218, USA*

²⁴*Institut für Experimentelle Kernphysik, Karlsruhe Institute of Technology, D-76131 Karlsruhe, Germany*

²⁵*Center for High Energy Physics: Kyungpook National University,*

Daegu 702-701, Korea; Seoul National University, Seoul 151-742,

Korea; Sungkyunkwan University, Suwon 440-746,

Korea; Korea Institute of Science and Technology Information,

Daejeon 305-806, Korea; Chonnam National University,

Gwangju 500-757, Korea; Chonbuk National University, Jeonju 561-756,

Korea; Ewha Womans University, Seoul, 120-750, Korea

²⁶*Ernest Orlando Lawrence Berkeley National Laboratory, Berkeley, California 94720, USA*

²⁷*University of Liverpool, Liverpool L69 7ZE, United Kingdom*

²⁸*University College London, London WC1E 6BT, United Kingdom*

²⁹*Centro de Investigaciones Energeticas Medioambientales y Tecnológicas, E-28040 Madrid, Spain*

³⁰*Massachusetts Institute of Technology, Cambridge, Massachusetts 02139, USA*

³¹*University of Michigan, Ann Arbor, Michigan 48109, USA*

³²*Michigan State University, East Lansing, Michigan 48824, USA*

³³*Institution for Theoretical and Experimental Physics, ITEP, Moscow 117259, Russia*

³⁴*University of New Mexico, Albuquerque, New Mexico 87131, USA*

³⁵*The Ohio State University, Columbus, Ohio 43210, USA*

³⁶*Okayama University, Okayama 700-8530, Japan*

³⁷*Osaka City University, Osaka 558-8585, Japan*

³⁸*University of Oxford, Oxford OX1 3RH, United Kingdom*

³⁹*Istituto Nazionale di Fisica Nucleare, Sezione di Padova, ^{jj}University of Padova, I-35131 Padova, Italy*

⁴⁰*University of Pennsylvania, Philadelphia, Pennsylvania 19104, USA*

⁴¹*Istituto Nazionale di Fisica Nucleare Pisa, ^{kk}University of Pisa,*

^{ll}University of Siena, ^{mm}Scuola Normale Superiore,

I-56127 Pisa, Italy, ⁿⁿINFN Pavia, I-27100 Pavia,

Italy, ^{oo}University of Pavia, I-27100 Pavia, Italy

⁴²*University of Pittsburgh, Pittsburgh, Pennsylvania 15260, USA*

⁴³*Purdue University, West Lafayette, Indiana 47907, USA*

⁴⁴*University of Rochester, Rochester, New York 14627, USA*

⁴⁵*The Rockefeller University, New York, New York 10065, USA*

⁴⁶*Istituto Nazionale di Fisica Nucleare, Sezione di Roma 1,*

^{pp}Sapienza Università di Roma, I-00185 Roma, Italy

⁴⁷Mitchell Institute for Fundamental Physics and Astronomy,
Texas A&M University, College Station, Texas 77843, USA

⁴⁸Istituto Nazionale di Fisica Nucleare Trieste, ⁴⁹Gruppo Collegato di Udine,

^{rr}University of Udine, I-33100 Udine, Italy, ^{ss}University of Trieste, I-34127 Trieste, Italy

⁴⁹University of Tsukuba, Tsukuba, Ibaraki 305, Japan

⁵⁰Tufts University, Medford, Massachusetts 02155, USA

⁵¹University of Virginia, Charlottesville, Virginia 22906, USA

⁵²Waseda University, Tokyo 169, Japan

⁵³Wayne State University, Detroit, Michigan 48201, USA

⁵⁴University of Wisconsin, Madison, Wisconsin 53706, USA

⁵⁵Yale University, New Haven, Connecticut 06520, USA

(Dated: May 20, 2021)

We report on a search for a dijet resonance in events with only two or three jets and large imbalance in the total event transverse momentum. This search is sensitive to the possible production of a new particle in association with a W or Z boson, where the boson decays leptonically with one or more neutrinos in the final state. We use the full data set collected by the CDF II detector at the Tevatron collider at a proton-antiproton center-of-mass energy of 1.96 TeV. These data correspond to an integrated luminosity of 9.1 fb^{-1} . We study the invariant mass distribution of the two jets with highest transverse energy. We find good agreement between data and standard model background expectations and measure the combined cross section for WW , WZ , and ZZ production to be $13.8_{-2.7}^{+3.0} \text{ pb}$. No significant anomalies are observed in the mass spectrum and 95% credibility level upper limits are set on the production rates of a potential new particle in association with a W or Z boson.

PACS numbers: 12.15.Ji, 12.38.Qk, 14.70.-e, 14.80.-j

I. INTRODUCTION

A study of the dijet invariant mass (m_{jj}) distribution in events with jet pairs produced in association with a W boson was performed by the CDF collaboration using $p\bar{p}$ collision data corresponding to an integrated luminosity of 4.3 fb^{-1} [1]. That analysis focused on W boson decays to $\ell\nu$ ($\ell = e$ or μ), where the presence of an identified electron (e) or muon (μ) was required in the event selection. Reference [1] reported evidence for a discrepancy with the standard model (SM) expectations, interpretable as an excess of events in the mass range of 120–160 GeV/c^2 corresponding to a significance of 3.2 standard deviations. In that study, the excess could be modeled with a Gaussian distribution, centered at 145 GeV/c^2 with an rms width of 14.3 GeV/c^2 , corresponding to the expected experimental m_{jj} resolution of the CDF II detector. The acceptance and selection efficiencies for events associated with such a dijet resonance were estimated by simulating Higgs boson (H) production in association with a W boson for a Higgs boson mass of 150 GeV/c^2 . Based on the assumption that the observed excess originated from a hypothetical new particle X with a branching fraction to quark pairs of one, the excess corresponded to a measured production cross section for $\sigma(p\bar{p} \rightarrow WX)$ of $3.1 \pm 0.8 \text{ pb}$ [2].

In this article, we present a search for a dijet resonance produced in association with a vector boson by studying the m_{jj} distribution from the two highest energy clusters of particles (jets) in events with only two or three detected jets and large imbalance in total event transverse momentum, indicative of the presence of undetected particles. We veto events containing one or more identified high- p_T leptons, in order to ensure that the sample is sta-

*Deceased

[†]With visitors from ^aUniversity of British Columbia, Vancouver, BC V6T 1Z1, Canada, ^bIstituto Nazionale di Fisica Nucleare, Sezione di Cagliari, 09042 Monserrato (Cagliari), Italy, ^cUniversity of California Irvine, Irvine, CA 92697, USA, ^dInstitute of Physics, Academy of Sciences of the Czech Republic, 182 21, Czech Republic, ^eCERN, CH-1211 Geneva, Switzerland, ^fCornell University, Ithaca, NY 14853, USA, ^gUniversity of Cyprus, Nicosia CY-1678, Cyprus, ^hOffice of Science, U.S. Department of Energy, Washington, DC 20585, USA, ⁱUniversity College Dublin, Dublin 4, Ireland, ^jETH, 8092 Zürich, Switzerland, ^kUniversity of Fukui, Fukui City, Fukui Prefecture, Japan 910-0017, ^lUniversidad Iberoamericana, Lomas de Santa Fe, México, C.P. 01219, Distrito Federal, ^mUniversity of Iowa, Iowa City, IA 52242, USA, ⁿKinki University, Higashi-Osaka City, Japan 577-8502, ^oKansas State University, Manhattan, KS 66506, USA, ^pBrookhaven National Laboratory, Upton, NY 11973, USA, ^qQueen Mary, University of London, London, E1 4NS, United Kingdom, ^rUniversity of Melbourne, Victoria 3010, Australia, ^sMuons, Inc., Batavia, IL 60510, USA, ^tNagasaki Institute of Applied Science, Nagasaki 851-0193, Japan, ^uNational Research Nuclear University, Moscow 115409, Russia, ^vNorthwestern University, Evanston, IL 60208, USA, ^wUniversity of Notre Dame, Notre Dame, IN 46556, USA, ^xUniversidad de Oviedo, E-33007 Oviedo, Spain, ^yCNRS-IN2P3, Paris, F-75205 France, ^zUniversidad Tecnica Federico Santa Maria, 110v Valparaiso, Chile, ^{aa}The University of Jordan, Amman 11942, Jordan, ^{bb}Universite catholique de Louvain, 1348 Louvain-La-Neuve, Belgium, ^{cc}University of Zürich, 8006 Zürich, Switzerland, ^{dd}Massachusetts General Hospital, Boston, MA 02114 USA, ^{ee}Harvard Medical School, Boston, MA 02114 USA, ^{ff}Hampton University, Hampton, VA 23668, USA, ^{gg}Los Alamos National Laboratory, Los Alamos, NM 87544, USA, ^{hh}Università degli Studi di Napoli Federico I, I-80138 Napoli, Italy

tistically independent from those used in other studies. The resulting final states are sensitive to $WX \rightarrow \ell\nu jj$ and $ZX \rightarrow \nu\bar{\nu}jj$ production and decay, where ℓ represents a hadronically-decaying τ lepton or an unidentified e or μ . We use the entire CDF $p\bar{p}$ collision data set corresponding to an integrated luminosity of 9.1 fb^{-1} .

The production of both WX and ZX states is of interest since many of the theoretical models proposed to explain the excess at $145 \text{ GeV}/c^2$ allow the hypothetical particle X to be produced in association with either a W boson or a Z boson. While studies on WX production are presented in Refs. [1, 3, 4], no studies focusing on ZX production have been reported to date. The search for WX and ZX production in events with jets and an imbalance of transverse energy is analogous to the search for WH and ZH production in the same final state [5], which has comparable sensitivity to that for the WH process reconstructed in the final state with a lepton and jets, but is based on an independent event sample.

II. DATA SAMPLE AND EVENT PRESELECTION

The data were collected by CDF II [7], a general-purpose detector used to study Tevatron $p\bar{p}$ collisions at a center-of-mass energy of 1.96 TeV. CDF II features a charged-particle tracking system consisting of a cylindrical open-cell drift chamber and silicon microstrip detectors immersed in a 1.4 T magnetic field parallel to the beam axis. Electromagnetic and hadronic calorimeters surrounding the tracking system measure the energies of charged and neutral particles. Drift chambers and scintillators located outside the calorimeter identify muons.

The calorimeter system consists of lead-scintillator sampling electromagnetic and iron-scintillator sampling hadronic calorimeters. The calorimeters comprise central barrel ($|\eta| \leq 1.1$) and plug ($1.1 \leq |\eta| \leq 3.6$) sections in pseudorapidity (η) space [8]. Calorimeter modules are arranged in a projective-tower geometry. Individual towers in the central barrel subtend 0.1 in $|\eta|$ and 15° in ϕ [8]. The sizes of the towers in the end plug calorimeter vary with $|\eta|$, subtending 0.1 in $|\eta|$ and 7.5° in ϕ at $|\eta| = 1.1$, and 0.5 in $|\eta|$ and 15° in ϕ at $|\eta| = 3.6$.

Jets are reconstructed from energy deposits in contiguous groups of calorimeter towers, using the JETCLU clustering algorithm [9] with a fixed cone size of $\Delta R \equiv \sqrt{(\Delta\eta)^2 + (\Delta\phi)^2} = 0.4$. Jet energies are corrected [10] for nonuniformities of the calorimeter response as a function of η , energy contributions from multiple $p\bar{p}$ interactions within the event, and the nonlinear response of the calorimeters. In contrast with the analysis described in Ref. [1], additional corrections are applied to the reconstructed jets in simulated events to more accurately model the energy scales of particle showers initiated by quarks and gluons. These corrections are obtained by comparing predicted and observed distributions of the transverse energy balance, $p_T(Z/\gamma) - E_T(\text{jet})$, from in-

dependent $Z+1$ jet and $\gamma+1$ jet event samples [11].

We consider events selected online due to the presence of large missing transverse energy [12]. We inclusively select events with $\cancel{E}_T > 45 \text{ GeV}$ and also the additional events with $\cancel{E}_T > 30 \text{ GeV}$ that contain two reconstructed jets. The event missing transverse energy is corrected offline for the presence of muons, which typically deposit only a fraction of their energy in the calorimeter, and reconstructed charged-particle tracks pointing at inactive regions of the detector. In order to only retain events for which the online selection is fully efficient, we require those selected for further analysis to have a corrected $\cancel{E}_T > 50 \text{ GeV}$.

We additionally require events to contain two or three reconstructed jets, where the two with the highest transverse energies [13], j_1 and j_2 , meet minimal threshold requirements of $E_T(j_1) > 35 \text{ GeV}$ and $E_T(j_2) > 25 \text{ GeV}$. Both jets are required to be reconstructed within the range $|\eta(j_i)| < 2$ and at least one of the two within $|\eta(j_i)| < 0.9$. We also require the two jets to be separated by $\Delta R(j_1, j_2) > 1$. Events containing only one additional jet with $E_T > 15 \text{ GeV}$ and $|\eta| < 2.4$ are not rejected, in order to increase acceptance for signal events with an extra jet originating from an initial- or final-state radiation or a hadronically-decaying τ lepton in the final state. Events containing an identified electron or muon with $p_T > 20 \text{ GeV}/c$ are rejected to maintain orthogonality with other search samples. Those events that satisfy all of the above criteria form the preselection sample used for this analysis.

III. BACKGROUND MODELING

We model SM background processes using a variety of Monte Carlo (MC) simulation programs. The diboson processes (WW , WZ , and ZZ) are generated with PYTHIA [14] incorporating γ^* contributions to the Z boson components for masses above $2 \text{ GeV}/c^2$. The normalization of simulated samples is extrapolated from next-to-leading order calculations [15, 16] with the γ^* and Z contributions restricted to the mass range between 40 and $140 \text{ GeV}/c^2$, yielding cross sections of 11.7 pb for WW , 3.6 pb for WZ , and 1.5 pb for ZZ processes, respectively. Top-quark production is generated assuming a top-quark mass of $172.5 \text{ GeV}/c^2$ [17]. Top-quark pair production is generated with PYTHIA, and its contribution is normalized to the approximate next-to-next-to-leading order cross section [18]. Single top-quark production is modeled using POWHEG [19] and normalized to the next-to-leading order cross sections [20, 21]. Production of a W or Z boson in association with parton jets is modeled by ALPGEN [22] incorporating PYTHIA to simulate parton showering and hadronization. Normalizations for predicted event rates associated with these processes are obtained from data.

We model multijet events from Quantum Chromodynamics processes, a major source of background in final

states with jets and \vec{E}_T , using a data-driven method. We define the missing transverse momentum $\vec{\cancel{p}}_T$, a variable similar to \vec{E}_T , as the negative vector sum of charged-particle transverse momenta from the reconstructed tracks in an event. As shown in Fig. 1, \vec{E}_T and $\vec{\cancel{p}}_T$ tend to be aligned for processes with neutrinos in the final state, such as diboson production, but aligned or antialigned in the data, which are dominated by multijet production. Because multijet processes result in final states with no neutrinos, observed \vec{E}_T necessarily originates from jet energy mismeasurements and therefore tends to point either in the same direction or direction opposite to the reconstructed \vec{E}_T of the mismeasured jet. Conversely, observed $\vec{\cancel{p}}_T$ in these events is generated from differences in the fractions of showering particles within each jet that are reconstructable as charged tracks, a mechanism uncorrelated with calorimeter energy mismeasurements. Hence, the directions of the observed \vec{E}_T and $\vec{\cancel{p}}_T$ in these events are in many cases different from one another. For events originating from dijet production, in which the two jets are produced opposite to one another, the azimuthal separation between the \vec{E}_T and $\vec{\cancel{p}}_T$ thus peaks in the regions near 0 or π . Hence, multijet background can be suppressed by rejecting events where $\Delta\phi(\vec{E}_T, \vec{\cancel{p}}_T) > \pi/2$, and rejected events can be used to model the multijet background contained within the selected data sample defined by $\Delta\phi(\vec{E}_T, \vec{\cancel{p}}_T) < \pi/2$. The applicability of this model is confirmed in data control regions [23] and supported by other measurements [5, 24, 25].

IV. ANALYSIS METHOD

Event preselection yields over 2 million candidate events, of which 94% are estimated to originate from multijet production. Requiring $\Delta\phi(\vec{E}_T, \vec{\cancel{p}}_T) < \pi/2$, reduces the multijet contribution by roughly a factor of two. To further reduce this background contribution, we require the azimuthal separation between the \vec{E}_T and each jet to satisfy $\Delta\phi(\vec{E}_T, \vec{j}_i) > 0.8$. We also require $\cancel{p}_T > 20$ GeV and large \cancel{E}_T significance ($\cancel{E}_T/\sqrt{\sum E_T} > 3.5$ GeV^{1/2}, where $\sum E_T$ is the scalar sum of transverse energies deposited in the calorimeter), as well as $\cancel{H}_T/\cancel{E}_T < 1.2$, where \cancel{H}_T is the magnitude of the negative vector sum of jet transverse energies. These additional selections reduce the multijet background by more than 99% and increase S/\sqrt{B} to 11.7 from 3.3, where S is the predicted number of SM diboson events and B is the predicted number of events from other SM processes in the selected samples.

To study the features of the m_{jj} distribution in the final event sample, we fit the observed distribution in data to the modeled distributions for the contributing background processes. Any contribution from WX and ZX production would appear as an additional narrow

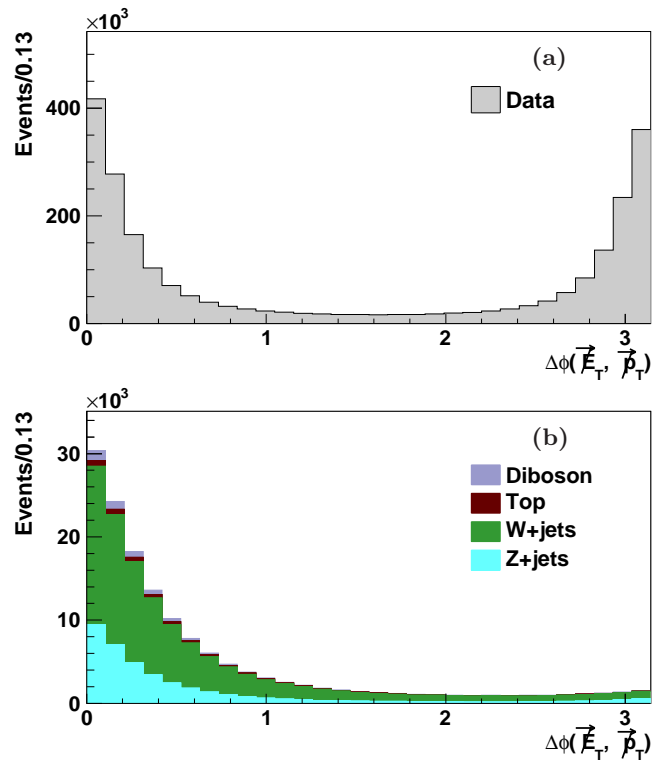


FIG. 1: Azimuthal separation between the \vec{E}_T and $\vec{\cancel{p}}_T$ for events that satisfy the preselection requirements. (a) The data distribution, for which 94% of events are estimated to originate from multijet production with observed \vec{E}_T and $\vec{\cancel{p}}_T$ that tend to be either aligned or antialigned. (b) Modeled distributions for the contributing SM processes leading to events containing final state neutrinos with observed \vec{E}_T and $\vec{\cancel{p}}_T$ that tend to be aligned.

structure overlapping the expected, resonant contribution from SM diboson production. First, we extract a measurement of diboson production by fitting the m_{jj} distribution for the relative event contributions from known SM processes and compare the result with theoretical predictions. We then allow for an additional Gaussian contribution from WX and ZX production and set 95% credibility level (C.L.) upper limits on the cross section for such processes using various theoretical constructs. The fits used to extract cross sections and upper limits are based on the Bayesian marginal likelihood method [26].

In the final fits, contributions from top-quark production are constrained based on theoretical predictions. Initial normalizations for the W/Z +jets and multijet background contributions are obtained by fitting the \cancel{E}_T distribution, which provides good discrimination between signal-like and background-like processes, using a χ^2 minimization technique. Figure 2 shows the fitted \cancel{E}_T distribution, where the W/Z +jets and multijet contributions are initially treated as unconstrained and determined from the fit. The resulting uncertainties on the multijet and W/Z +jets contributions originating from this proce-

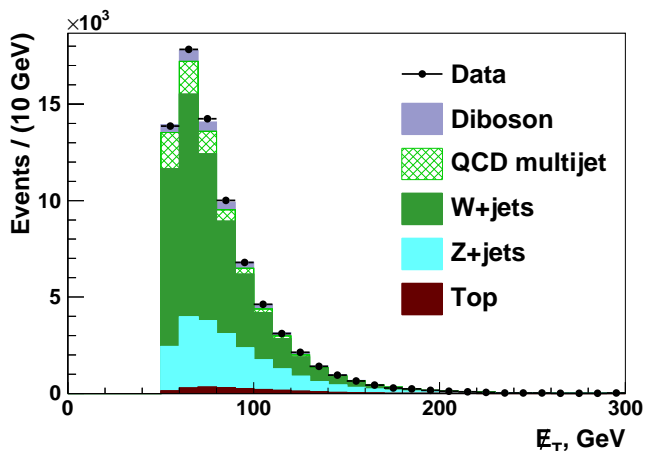


FIG. 2: Missing transverse energy distribution of events satisfying all selection criteria with fitted SM contributions overlaid. The last bin includes overflow events with $E_T > 300$ GeV.

ture are 19% and 3%, respectively. Table I summarizes predicted event contributions to the final event sample from diboson production and other SM background processes, which are taken as inputs to the final fits performed on the observed m_{jj} spectrum. Figure 3 shows comparisons of predicted and observed distributions for $E_T(j_1)$, $E_T(j_2)$, and $\Delta\phi(j_1, j_2)$, variables strongly correlated with dijet invariant mass, from events in the final sample.

TABLE I: Predicted number of events from each contributing SM process in the final event sample and the total number of observed events, where the normalization of W/Z +jets and multijet background processes are obtained from a fit to the E_T distribution. Uncertainties include statistical and systematic contributions.

Process	Yield
WW	1850 ± 170
WZ	670 ± 60
ZZ	380 ± 30
Top quark	2040 ± 190
W +jets	46170 ± 1390
Z +jets	19710 ± 590
multijet	6280 ± 1190
Total expected	77100 ± 2320
Data	77149

When performing the maximum likelihood fits, we consider several sources of systematic uncertainties, included as constraints in the likelihood. Sources that affect predicted event yields for modeled background contributions are referred to as rate uncertainties. Dominant rate uncertainties include those on the normalizations obtained from data to constrain multijet (19%) and W/Z +jets (3%) contributions. Uncertainties associated with theoretical cross section calculations (6–7%) and the sample

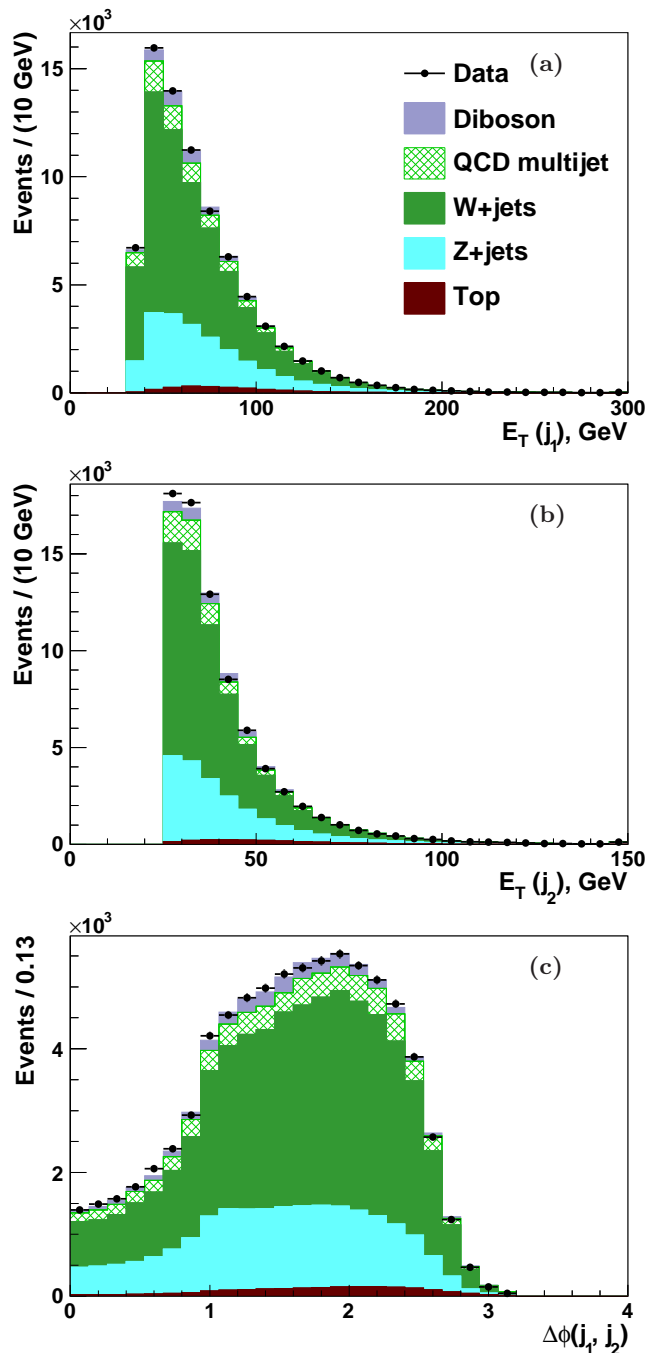


FIG. 3: Distributions of (a) $E_T(j_1)$, (b) $E_T(j_2)$, and (c) $\Delta\phi(j_1, j_2)$ for events satisfying all selection criteria with fitted SM contributions overlaid. The last bins of the distributions shown in (a) and (b) include overflow events with $E_T(j_1) > 300$ GeV and $E_T(j_2) > 150$ GeV, respectively.

luminosity measurement [27] (6%), which affect predicted background process event rates taken directly from simulation, are also included. In addition, uncertainty sources such as jet energy scale [10] (1.4–13%), parton density functions (2%), efficiency of lepton veto requirements (2%), and measured trigger efficiencies (0.4–1.5%) that

affect simulated detector event acceptances are incorporated on both the signal and background contributions.

We also incorporate the effects of systematic uncertainty sources, which result in variations in the shapes of modeled m_{jj} distributions for the contributing processes. For those processes modeled via simulation, we account for potential variations in the shape of the m_{jj} distribution originating from jet energy scale uncertainties. Uncorrelated uncertainties on the simulated energy scales for jets originating from quarks (3%) and gluons (6%) are considered separately. In the case of the W/Z +jets background contribution, shape uncertainties resulting from factor of two changes to the nominal Q^2 scale used in the perturbative expansion for calculating matrix elements in the ALPGEN generator are also incorporated. Finally, for the modeled m_{jj} distribution from multijet production, we obtain shape uncertainties by varying the normalization of the modeled contributions from other processes, which are subtracted from the data distribution obtained from events with $\Delta\phi(\cancel{E}_T, \cancel{p}_T) > \pi/2$.

V. RESULTS

A. Diboson Measurement

We fit the distribution of m_{jj} from the two highest-energy jets in events passing all selection criteria to extract a cross section measurement for diboson production. We take SM values for the relative production rates of the WW , WZ , and ZZ processes in order to obtain a single m_{jj} template corresponding to combined diboson production. The diboson contribution is allowed to float freely by assuming a flat, non-negative prior probability for the total cross section. The unit Gaussian priors of the nuisance parameters are centered on zero and truncated whenever the value results in a nonphysical prediction. Figure 4 shows the fitted m_{jj} distribution and a comparison of the fitted diboson contribution against the data after subtracting the other background contributions obtained from the fit. The inclusive cross section $\sigma(p\bar{p} \rightarrow VV)$, where $VV = WW + WZ + ZZ$, is measured to be $13.8^{+3.0}_{-2.7}$ pb for γ^* and Z contributions restricted to the mass range between 40 and 140 GeV/c^2 , which is in good agreement with the SM prediction of 16.8 ± 1.0 pb.

B. Limits on Dijet-Resonance Cross Sections

To search for WX and ZX production, we perform a second fit, normalizing diboson contributions to their theoretical expectation and assuming 6% uncertainties on their theoretical cross sections. We allow for an additional signal contribution, modeled assuming a Gaussian distribution, centered at 145 GeV/c^2 with an rms width of 14.3 GeV/c^2 , in accordance with Ref. [1]. To be consistent with the cross section reported in Ref. [2], we model

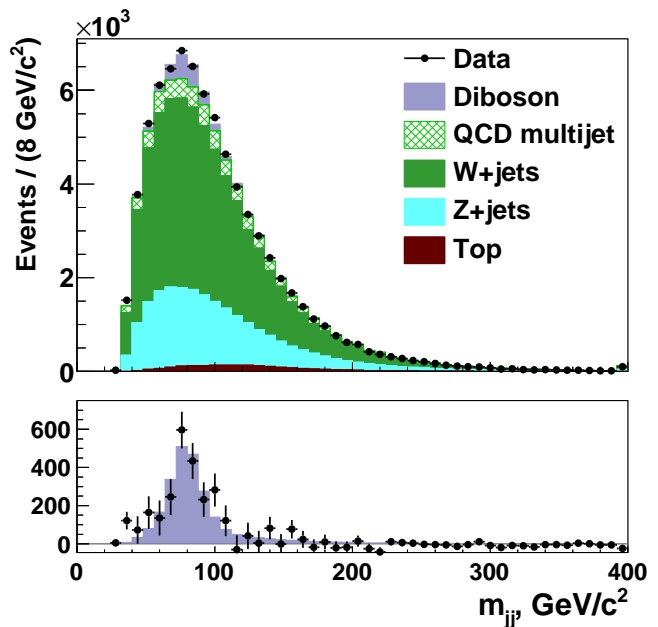


FIG. 4: Dijet invariant mass distribution with fit results overlaid for events passing all selection criteria (top) and the same background-subtracted distribution with the fitted diboson contribution overlaid (bottom). The last bin includes overflow events with $m_{jj} > 400 \text{ GeV}/c^2$.

the signal acceptance from simulated Higgs boson production in association with a W or Z boson for a Higgs boson mass of 150 GeV/c^2 to extract cross section limits. As the relative production rate of WX and ZX varies among theoretical models, we set upper limits on combined production ($\sigma_{\text{tot}} = \sigma_{WX} + \sigma_{ZX}$) for three scenarios: (1) $\sigma_{WX} = 100\%$ and $\sigma_{ZX} = 0\%$, (2) $\sigma_{WX} = 76\%$ and $\sigma_{ZX} = 24\%$, and (3) $\sigma_{WX} = 61\%$ and $\sigma_{ZX} = 39\%$. The second and third scenarios correspond approximately to the relative SM rates for WZ/ZZ and WH/ZH production, respectively.

TABLE II: Median expected, assuming the background only hypothesis, and observed 95% C.L. upper limits on the combined $WX+ZX$ cross section (σ_{tot}) under various hypotheses for the relative magnitudes of σ_{WX} and σ_{ZX} .

Signal scenario	Expected	Observed
	upper limit	upper limit
	on σ_{tot}	on σ_{tot}
$\sigma_{WX}/\sigma_{\text{tot}} = 1.00, \sigma_{ZX}/\sigma_{\text{tot}} = 0.00$	1.31 pb	2.20 pb
$\sigma_{WX}/\sigma_{\text{tot}} = 0.76, \sigma_{ZX}/\sigma_{\text{tot}} = 0.24$	1.02 pb	1.72 pb
$\sigma_{WX}/\sigma_{\text{tot}} = 0.61, \sigma_{ZX}/\sigma_{\text{tot}} = 0.39$	0.90 pb	1.52 pb

The observed and median expected, assuming the background only hypothesis, 95% C.L. upper limits on the combined cross section for WX and ZX production (σ_{tot}) obtained from the fit are shown in Table II for each of the three scenarios. Figure 5 shows a comparison of these limits relative to expectations for each sce-

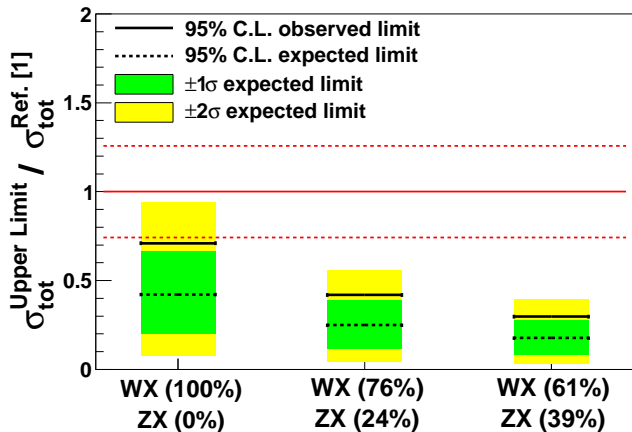


FIG. 5: Observed and median expected, assuming the background only hypothesis, 95% C.L. upper limits on the combined $WX+ZX$ cross section (σ_{tot}) divided by the most likely value extrapolated from the excess reported in Ref. [1] for each of the three signal scenarios. The measurement uncertainty associated with the WX cross section [2] assigned to the excess described in Ref. [1] is indicated by the light (red) dashed lines.

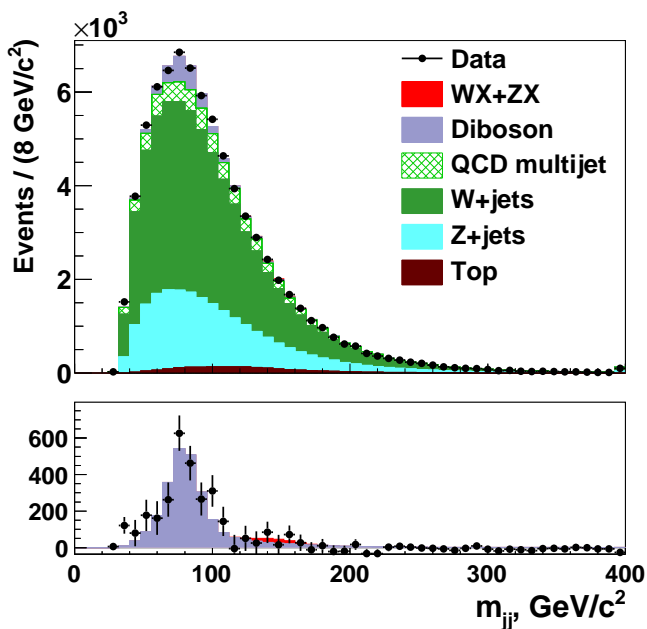


FIG. 6: Dijet invariant mass distribution with fit results overlaid for events passing all selection criteria (top) and the same background-subtracted distribution with the fitted contributions from diboson and combined WX/ZX production overlaid (bottom). The last bin includes overflow events with $m_{jj} > 400$ GeV/c^2 .

nario based on the WX production cross section extrapolated from the observed excess reported in Ref. [1]. The

one standard deviation uncertainties associated with this measured cross section are indicated by the light (red) dashed lines. In all scenarios, the most likely value of the combined WX and ZX production cross section corresponding to the observed excess is excluded at the 95% C.L. Figure 6 shows the fitted m_{jj} distribution and a comparison of the combined fitted contributions of dibosons and WX/ZX production against the data, with other background contributions as obtained from the fit subtracted.

VI. CONCLUSION

We study the dijet invariant mass distribution in events with energetic jets and large missing transverse energy using the full CDF II data set corresponding to an integrated luminosity of 9.1 fb^{-1} . A fit of the observed distribution to modeled distributions for the expected contributions of SM production processes gives a measured cross section for combined diboson production of $\sigma(p\bar{p} \rightarrow VV) = 13.8^{+3.0}_{-2.7} \text{ pb}$, in good agreement with the SM prediction of $16.8 \pm 1.0 \text{ pb}$. In the absence of a significant deviation from the background expectation in the dijet invariant mass spectrum, we set 95% C.L. upper limits on the combined cross section for the production of a new particle X in association with a W or Z boson, under several hypotheses for the relative production rates of WX and ZX . For each of these hypotheses, we exclude at 95% C.L. the most likely value of the combined $WX+ZX$ cross section corresponding to the excess observed in Ref. [1].

VII. ACKNOWLEDGMENTS

We thank the Fermilab staff and the technical staffs of the participating institutions for their vital contributions. This work was supported by the U.S. Department of Energy and National Science Foundation; the Italian Istituto Nazionale di Fisica Nucleare; the Ministry of Education, Culture, Sports, Science and Technology of Japan; the Natural Sciences and Engineering Research Council of Canada; the National Science Council of the Republic of China; the Swiss National Science Foundation; the A.P. Sloan Foundation; the Bundesministerium für Bildung und Forschung, Germany; the Korean World Class University Program, the National Research Foundation of Korea; the Science and Technology Facilities Council and the Royal Society, UK; the Russian Foundation for Basic Research; the Ministerio de Ciencia e Innovación, and Programa Consolider-Ingenio 2010, Spain; the Slovak R&D Agency; the Academy of Finland; the Australian Research Council (ARC); and the EU community Marie Curie Fellowship contract 302103.

-
- [1] T. Aaltonen *et al.*, (CDF Collaboration), Phys. Rev. Lett. **106**, 171801 (2011).
- [2] V. Cavaliere, PoS EPS-HEP2011 (2011) 215.
- [3] V.M. Abazov *et al.*, (D0 Collaboration), Phys. Rev. Lett. **107**, 011804 (2011).
- [4] S. Chatrchyan *et al.* (CMS Collaboration), Phys. Rev. Lett. **109**, 251801 (2012).
- [5] T. Aaltonen *et al.*, (CDF Collaboration), Phys. Rev. Lett. **109**, 111805 (2012).
- [6] T. Aaltonen *et al.*, (CDF Collaboration), Phys. Rev. Lett. **109**, 111804 (2012).
- [7] D. Acosta *et al.*, (CDF Collaboration), Phys. Rev. D **71**, 032001 (2005).
- [8] CDF uses a cylindrical coordinate system with the z axis along the proton beam axis. Pseudorapidity is $\eta = -\ln(\tan(\theta/2))$, where θ is the polar angle relative to the proton beam direction, and ϕ is the azimuthal angle while p_T and E_T are defined as $p_T = |p| \sin \theta$, $E_T = E \sin \theta$.
- [9] F. Abe *et al.* (CDF collaboration), Phys. Rev. D **45**, 001448 (1992).
- [10] A. Bhatti *et al.*, Nucl. Instrum. Methods A **566**, 375 (2006).
- [11] T. Aaltonen *et al.*, (CDF Collaboration), submitted to Phys. Rev. D, arXiv:1310.0086 (2013).
- [12] Missing transverse energy, \vec{E}_T , is defined as the magnitude of the vector $\vec{E}_T = -\sum_i E_T^i \vec{n}_i$ where E_T^i is the magnitude of transverse energy contained in each calorimeter tower i , and \vec{n}_i is the unit vector from the interaction vertex to the tower in the transverse (x, y) plane.
- [13] Jet transverse energy, E_T , is defined as $\sum_{i=0}^N E_i \sin \theta_{jet}$ where E_i is the energy deposited in each of N calorimeter towers, and θ is the polar angle of the reconstructed jet cluster.
- [14] T. Sjostrand, S. Mrenna, and P. Skands, J. High Energy Phys. 05 (2006) 026.
- [15] J. M. Campbell and R. K. Ellis, Phys. Rev. D **60**, 113006 (1999).
- [16] J. M. Campbell and R. K. Ellis, Phys. Rev. D **62**, 114012 (2000).
- [17] T. Aaltonen *et al.* (CDF and D0 Collaborations), Phys. Rev. D **86**, 092003 (2012).
- [18] U. Langenfeld, S. Moch, and P. Uwer, Phys. Rev. D **80**, 054009 (2009).
- [19] S. Alioli, P. Nason, C. Oleari, and E. Re, J. High Energy Phys. 06 (2010) 043.
- [20] B. W. Harris, E. Laenen, L. Phaf, Z. Sullivan, and S. Weinzierl, Phys. Rev. D **66**, 054024 (2002).
- [21] Z. Sullivan, Phys. Rev. D **70**, 114012 (2004).
- [22] M. L. Mangano, F. Piccinini, A. Polosa, M. Moretti, and R. Pittau, J. High Energy Phys. 07 (2003) 001.
- [23] M. Bentivegna, D. Bortoletto, Q. Liu, F. Margaroli, and K. Potamianos, arXiv:1205.4470 (2012).
- [24] T. Aaltonen *et al.* (CDF Collaboration), Phys. Rev. D **81**, 072003 (2010).
- [25] T. Aaltonen *et al.* (CDF Collaboration), Phys. Rev. Lett. **107**, 191803 (2011).
- [26] T. Aaltonen *et al.* (CDF Collaboration), Phys. Rev. D **82**, 112005 (2010).
- [27] D. Acosta *et al.*, Nucl. Instrum. Methods A **494**, 57 (2002).